DEPENDENCE OF SURFACE RESISTANCE ON N-DOPING LEVEL*

D. Gonnella†, F. Furuta, M. Ge, J. Kaufman, P.N. Koufalis, M. Liepe, and J.T. Maniscalco

CLASSE, Cornell University, Ithaca, NY 14853, USA

Abstract

Nitrogen-doping has become a standard tool for reaching high quality factors in SRF cavities in the medium field region at 2 K. This high Q has been shown to be a result of lowering of the temperature dependent BCS resistance. Here we show that this lowering of the BCS resistance is due to interstitial nitrogen in the niobium lowering the mean free path. The BCS resistance extracted from experimental data is shown to be consistent with theoretical predictions from BCS theory; that there is an optimal doping of which the mean free path is lowered to about half the intrinsic coherence length. These results provide insight into understanding the mechanisms behind nitrogen-doping and allow us to more accurately predict doping parameters to reach optimal cavity performance.

INTRODUCTION

New accelerators such as LCLS-II at SLAC require the SRF cavities in the linac to operate at significantly higher intrinsic quality factors, Q_0, than have been achieved in large scale projects in the past. In order to meet the ambitious specifications of 2.7×10^{10} at 16 MV/m and 2.0 K [1], nitrogen-doping of the cavities will be used as a surface preparation technique. Nitrogen-doping consists of treating the cavities in a UHV furnace at high temperature in a low nitrogen atmosphere. This has been shown to result in higher Q_0 at low fields than standard cavities and an anti-Q slope which results in the Q_0 increasing further into the medium field region [2, 3]. This change in Q_0 has been directly attributed to a lowering of the temperature-dependent BCS resistance, R_{BCS}. While this performance has been achieved consistently, the underlying physics of how nitrogen affects the performance was not well understood. Here we present on work completed on single-cell cavities at Cornell to systematically study the effect of nitrogen-doping on R_{BCS}.

CAVITIES PREPARED AND TESTED

For the purposes of these studies, 5 single-cell 1.3 GHz ILC shaped cavities were used. These five cavities received different levels of nitrogen-doping for a total of 10 cavity preparations. 6 of the preparations were doping at 800 °C for 20 minutes followed by a 30 minute anneal and then various amounts of final vertical electropolish (VEP) [4] between 6 and 40 μm. Three of the the remaining preparations were doped at 900°C for 20 minutes followed by a 30 minute anneal and then varying amounts of final VEP between 6 and 18 μm. The final preparation was a doping at 990°C for 5 minutes followed by a final VEP of 5 μm. For each of these cavities the following was measured: Q_0 versus E_{acc} at various temperatures below 2.1 K up to quench, Q_0 versus temperature at low fields from 4.2 to 1.6 K, and resonance frequency versus temperature near T_c. This allowed for R_{BCS} to be extracted at 5 MV/m and 16 MV/m (the field of interest to LCLS-II) along with the mean free path via BCS fitting [5, 6]. For a full list of the extracted material properties and R_{BCS} values see [7].

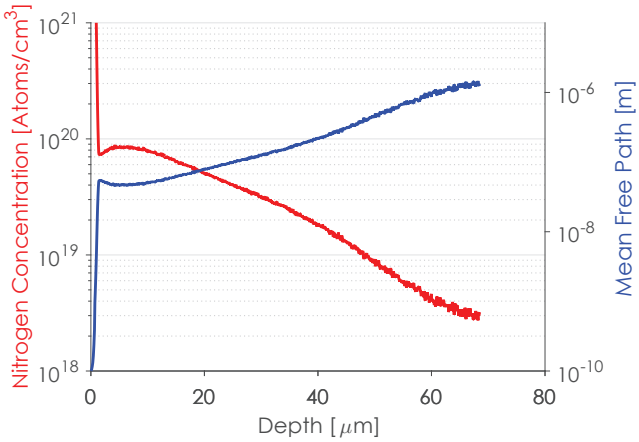

Figure 1: Nitrogen concentration from SIMS on a sample of niobium doped at 800°C for 20 minutes in 60 mTorr of nitrogen gas followed by a 30 minute anneal. Also shown is the calculated mean free path from the nitrogen concentration.

NITROGEN-DOPING EFFECT ON MEAN FREE PATH

Niobium samples were doped along with the cavities at 800°C for analysis with Secondary Ion Mass Spectroscopy (SIMS). The results of this measurement are shown in Fig. 1. Also shown is the calculated mean free path from the nitrogen concentration by

$$\ell = \frac{\sigma}{[5.2\times10^{-8}\Omega\cdot\,\mathrm{m}]\cdot c}, \qquad (1)$$

with ℓ the mean free path, $\sigma = 0.37\times10^{-15}\ \Omega\cdot m^2$ [8], and c the atomic percentage of nitrogen in the niobium. What we can see from Fig. 1 is that the mean free path of the niobium is strongly affected by the doping process for a significant depth into the material. This change in mean free path will have a drastic impact on R_{BCS} which is heavily dependent on material properties [9].

* Work supported by the US DOE and the LCLS-II High Q0 Program and NSF Grant PHY-1416318

† dg433@cornell.edu

ISBN 978-3-95450-147-2

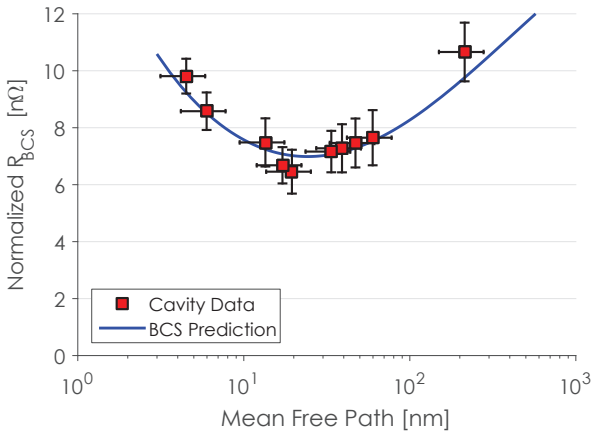

Figure 2: R_{BCS} at 5 MV/m and 2.0 K (normalized for the differences in energy gap) for the cavities tested as a function of mean free path. There is good agreement between the experimental data and the prediction from BCS theory at low fields. Low field improvement in Q_0 in nitrogen-doped cavities is due to lowering of the mean free path to bring R_{BCS} near the minimum at $\ell \approx \xi_0/2 \approx 20$ nm.

LOWERING OF R_{BCS} AT LOW FIELDS

The dependence of R_{BCS} on material properties such as the mean free path can be calculated from BCS theory [10] using a code developed by Halbritter called SRIMP [11] for small RF fields. BCS theory predicts a minimum at mean free paths of approximately half the coherence length. Figure 2 shows R_{BCS} at 5 MV/m and 2.0 K (normalized for differences in the energy gap) for the cavities tested as a function of their extracted mean free path along with the prediction from BCS theory. There is a clear minimum in the experimental data, corresponding to predicted minimum in BCS theory at $\ell \approx \xi_0/2 \approx 20$ nm. We can therefore say concretely that the low field improvement in Q_0 in nitrogen-doped cavities is a result of the lowering of the mean free path closer to the minimum as predicted by BCS theory.

STRENGTH OF THE ANTI-Q SLOPE

The second effect observed in nitrogen-doped cavities is the presence of an anti-Q slope which further decreases R_{BCS} in the medium field region.

Logarithmic Dependence with Field

This anti-Q slope in the medium field region (~20 – 100 mT) roughly follows a logarithmic dependence on the magnitude of the RF field [3]. Figure 3 shows R_{BCS} versus B_{pk} at 2.0 K for two of the nitrogen-doped cavities tested along with logarithmic fits to their anti-Q slope. While there is no theoretical basis for fitting to a logarithm, it provides a "quick and dirty" method for quantifying the anti-Q slope.

Anti-Q Slope vs Mean Free Path

The logarithmic fitting described in the previous section was applied to all of the nitrogen-doped cavities presented

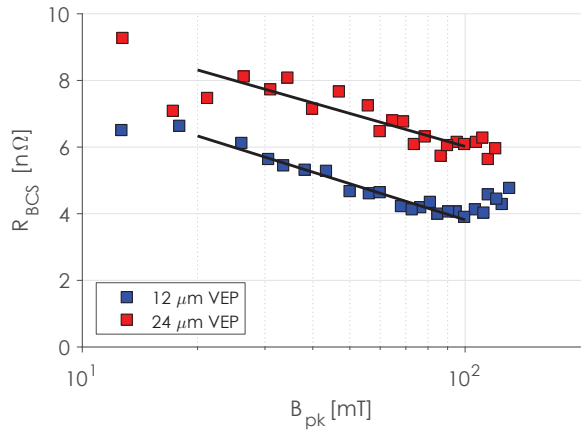

Figure 3: R_{BCS} versus B_{pk} for two nitrogen-doped cavities tested at 2.0 K. The anti-Q slope region is well described by a logarithmic dependence on B_{pk}.

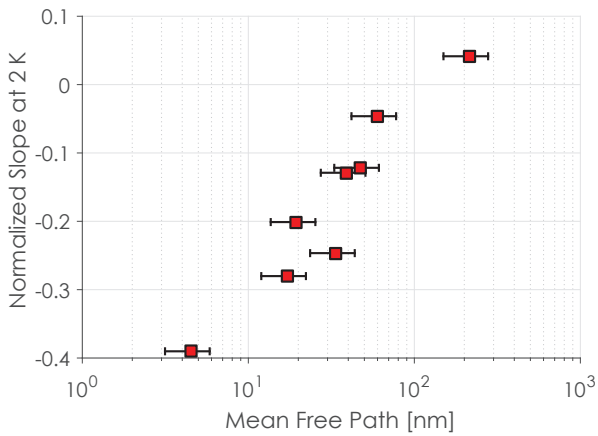

Figure 4: Slope of logarithmic fit to the anti-Q slope region at 2.0 K normalized to R_{BCS} at low fields for the nitrogen-doped cavities tested versus their mean free paths. Longer mean free path leads to a weaker anti-Q slope.

in this paper. The slope of the fit (on a log scale) at 2.0 K, normalized to R_{BCS} at low fields, versus mean free path is shown in Fig. 4. There is a clear trend that longer mean free paths lead to a smaller anti-Q slope (less negative in Fig. 4). This behavior manifests as roughly logarithmic. At very large mean free paths, as the cavity approaches an un-doped cavity, the anti-Q slope completely disappears and the medium field Q slope which is usually present in standard preparation cavities returns.

The relative strength of the anti-Q slope is most interestingly not strongly temperature dependent. Figure 5 shows the slope of the logarithmic fits normalized to R_{BCS} at low fields as a function of temperature for the cavities doped at 800°C. After 40 μm removal, the cavity shown in yellow is effectively un-doped and no longer has an anti-Q slope at any temperature. While the other cavities show an anti-Q slope, the strength of it is almost completely temperature independent.

ISBN 978-3-95450-147-2

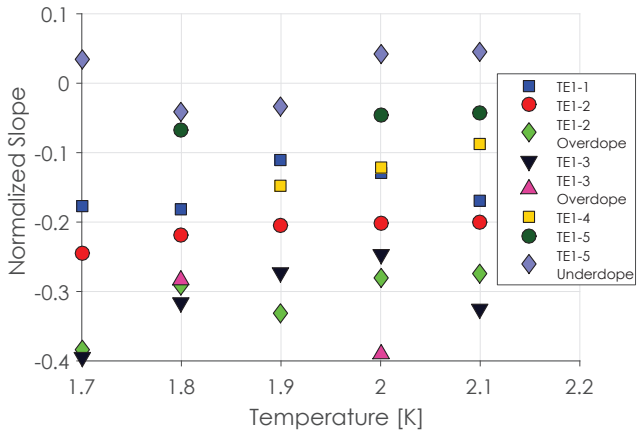

Figure 5: Slope of the logarithmic fit to the anti-Q slope region as a function of temperature normalized to R_{BCS} at low fields for the cavities doped at 800°C. Anti-Q slope is mostly temperature independent for all of the cavities tested.

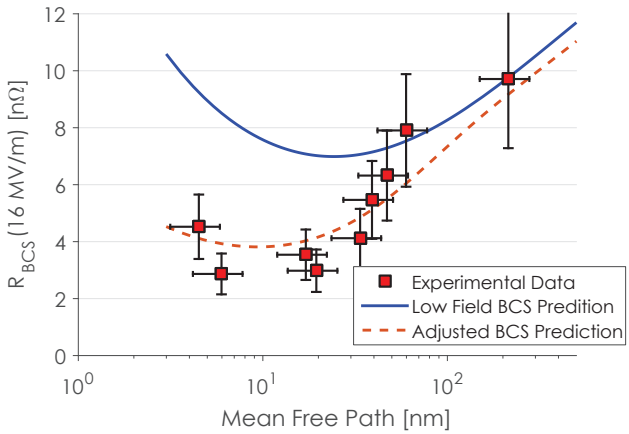

Figure 6: 2.0 K R_{BCS} at 16 MV/m versus mean free path for the cavities tested. Also shown in the low field BCS prediction and an adjustment to the low field prediction based on the logarithmic fitting to the anti-Q slope and Fig. 4.

OPTIMIZED R_{BCS}

With an understanding of R_{BCS} at low fields as discussed previously and a better understanding of how the anti-Q slope manifests with changes in mean free path and temperature, it is now useful to discuss the optimal doping level for minimizing R_{BCS}. Because nitrogen-doped cavities will be applied to machines such as LCLS-II, the most important figure of merit is R_{BCS} at the operating gradient (16 MV/m for LCLS-II). Figure 6 shows R_{BCS} at 16 MV/m versus mean free path for the cavities tested. The two "dirtiest" cavities shown quenched at lower fields than 16 MV/m. In order to complete the optimization, the anti-Q slope was extended for these cavities assuming a logarithmic dependence on the RF field magnitude. Also shown in Fig. 6 is the low field prediction from BCS theory. Unsurprisingly, low-field BCS theory does not predict the correct R_{BCS} (16 MV/m) for the cavities which have a strong anti-Q slope (in the dirty limit). There is good agreement however at long mean free paths where the anti-Q slope is small. This makes sense since R_{BCS} is roughly field independent for those cavities. Lastly shown in Fig. 6 is an adjustment to the low field prediction from BCS theory. This adjustment was done by scaling R_{BCS} at low fields with the anti-Q slope measured as a function of mean free path (as in Fig. 4). This adjustment produces very good agreement with the experimental data. Most interestingly though, this shifts the expected minimum in R_{BCS} from ~20 nm to ~10 nm. This suggests that in order to most efficiently minimize R_{BCS} at operating fields (such as 16 MV/m), stronger doping should be employed in order to reach mean free paths of 10 nm.

CONCLUSIONS

This work represents significant progress towards understanding the mechanisms behind nitrogen-doping's success. Low field improvement in Q_0 over cavities prepared with standard preparation techniques is due to a lowering of the mean free path via interstitial nitrogen acting as defects in the niobium. In fact nitrogen-doped cavities can have mean free paths close to those for which minimum R_{BCS} is predicted by BCS theory and the in fact closely follow the theoretical prediction made by BCS theory. The anti-Q slope present in nitrogen-doped cavities can be described by a logarithmic dependence on the magnitude of the RF field. The strength of the anti-Q slope decreases with lighter dopings and is not strongly dependent on temperature. Finally, R_{BCS} at 16 MV/m is optimized at mean free paths of ~10 nm. This minimum is close to the minimum as predicted by BCS theory at low fields but shifted further towards the dirty limit and is usually obtained with moderate to heavy doping levels.

Nitrogen-doping continues to show promise as a viable cavity preparation technique for future machines. While we have presented significant steps forward in terms of understanding how nitrogen-doping relates to improved performance, there is still much to study especially in the area of the anti-Q slope. Future work will focus on further studying this region and comparing experimental results with theoretical predictions and on studying the effect of doping SRF cavities with other atoms besides nitrogen.

REFERENCES

[1] J.N. Galayda. The LCLS-II Project. In *Proceedings of IPAC 2014, Dresden, Germany*, pages 935–937, Dresden, Germany, June 2014. JACoW.

[2] A. Grassellino, A. Romanenko, D. Sergatskov, O. Melnychuk, Y. Trenikhina, A. Crawford, A. Rowe amd M. Wong, T. Khabiboulline, and F. Barkov. Nitrogen and argon doping of niobium for superconducting radio frequency cavities: a pathway to highly efficient accelerating structures. *Superconductor Science and Technology*, 26(102001), 2013.

[3] Dan Gonnella, Mingqi Ge, Fumio Furuta, and Matthias Liepe. Nitrogen Treated Cavity Testing at Cornell. In *Proceedings*

ISBN 978-3-95450-147-2

of LINAC 2014, Geneva, Switzerland, number THPP016, Geneva, Switzerland, September 2014. JaCoW.

[4] F. Furuta, G. Hoffstaetter, M. Ge, M. Liepe, and B. Elmore. Multi-Cell VEP Results: High Voltage, High Q, and Localized Temperature Analysis. In *Proceedings of IPAC 2012, New Orleans, LA, USA*, number TUPPR045, pages 1918–1920, New Orleans, LA, USA, May 2012. JaCoW.

[5] Nicholas Valles. *Pushing the Frontiers of Superconducting Radio Frequency Science: From the Temperature Dependence of the Superheating Field of Niobium to Higher-Order Mode Damping in Very High Quality Factor Accelerating Structures*. PhD Thesis, Cornell University, 2013.

[6] S. Meyers, S. Posen, and M. Liepe. Analysis of Systematic and Random Error in SRF Material Parameter Calculations. In *Proceedings of Linac 2014*, number TUPP018, Geneva, Switzerland, September 2014. JaCoW.

[7] Daniel Gonnella. *The Fundamental Science of Nitrogen-Doping of Niobium Superconducting Cavities*. Thesis, Cornell University, 2016.

[8] B.B. Goodman and G. Kuhn. Influence of Extended Defects on the Superconductive Properties of Niobium. *J. Phys. Paris*, 29(240), 1968.

[9] Hasan Padamsee, Jens Knobloch, and Tom Hays. *RF superconductivity for accelerators*. Wiley, New York, 1998.

[10] J. Bardeen, L.N. Cooper, and J.R. Schrieffer. Microscopic Theory of Superconductivity. *Physical Review*, 106:162–164, 1957.

[11] J. Halbritter. FORTRAN-Program for the Computation of the Surface Impedance of Superconductors. *KAROLA - OA-Volltextserver des Forschungszentrums Karlsruhe [http://opac.fzk.de:81/oai/oai-2.0.cmp.S] (Germany)*, (3/70-6), 1970.

ISBN 978-3-95450-147-2